

Article

IoMT-Based Automated Diagnosis of Autoimmune Diseases Using MultiStage Classification Scheme for Sustainable Smart Cities

Divya Biligere Shivanna ¹, Thompson Stephan ^{1,*} , Fadi Al-Turjman ² , Manjur Kolhar ³ and Sinem Alturjman ⁴

¹ Department of Computer Science and Engineering, M. S. Ramaiah University of Applied Sciences, Bengaluru 560054, Karnataka, India

² Artificial Intelligence Engineering Department, AI and Robotics Institute, Near East University, Mersin 10, 99010 Nicosia, Turkey

³ Department of Computer Science, College of Arts and Science, Prince Sattam Bin Abdulaziz University, Al-Kharj 11990, Saudi Arabia

⁴ Research Center for AI and IoT, Faculty of Engineering, University of Kyrenia, Mersin 10, 99320 Kyrenia, Turkey

* Correspondence: thompsoncse@gmail.com

Abstract: The resolution of complex medical diagnoses using pattern recognition requires an artificial neural network-based expert system to automate autoimmune disease diagnosis in blood samples. This process is done using image-based computer-aided diagnosis (CAD) to reduce errors in the diagnosis process. This paper describes a Multistage Classification Scheme (MSCS), which uses antinuclear antibody (ANA) tests to identify and classify the existence of autoantibodies in the blood serum that bind to antigens found in the nuclei of mammalian cells. The MSCS classified HEp-2 cells into three stages by using Binary Tree (BT), Artificial Neural Network (ANN), and Support Vector Machine (SVM) as basic blocks. The Indirect Immunofluorescence (IIF) technique is used in the ANA test with Human Epithelial type-2 (HEp-2) cells as substrates. The efficiency of the proposed methodology is assessed using the dataset of ICPR 2016. The intermediate cells (IMC) and positive cells (PC) were separated in Stage 1 prior to preprocessing based on their total strength, and special preprocessing is applied to intermediate cells for improved output, and positive cells are subjected to mild preprocessing. The mean class accuracy (MCA) was 84.9% for intermediate cells and 95.8% for positive cells, although the carefully picked 24 features and SVM classifier were applied. ANN showed better performance by adjusting the weights using the SCGBP algorithm. So, the MCA is 88.4% and 97.1% for intermediate and positive cells, respectively. BT had an MCA of 95.3% for intermediate and 98.6% for positive. In Stage 2, the meta learners BT2, ANN2, and SVM2 were trained for an augmented feature set (24 + 3 results from base learners). Therefore, the performance of BT2, ANN2, and SV M2 was increased by 1.8%, 4.5%, and 4.1% as compared to Stage 1. In Stage 3, the final prediction was performed by majority voting among the results of the three meta learners to achieve 99.1% MCA. The proposed algorithm can be embedded into a CAD framework built for the ANA examination. The proposed model will improve operational efficiency, decrease medical expenses, expand accessibility to healthcare, and improve patient safety in the sector, enabling enterprises to lower unplanned downtime, develop new products or services, increase operational effectiveness, and enhance risk management.



Citation: Shivanna, D.B.; Stephan, T.; Al-Turjman, F.; Kolhar, M.; Alturjman, S. IoMT-Based Automated Diagnosis of Autoimmune Diseases Using MultiStage Classification Scheme for Sustainable Smart Cities. *Sustainability* **2022**, *14*, 13891. <https://doi.org/10.3390/su142113891>

Academic Editor: Andreas Kanavos

Received: 24 September 2022

Accepted: 19 October 2022

Published: 26 October 2022

Publisher's Note: MDPI stays neutral with regard to jurisdictional claims in published maps and institutional affiliations.



Copyright: © 2022 by the authors. Licensee MDPI, Basel, Switzerland. This article is an open access article distributed under the terms and conditions of the Creative Commons Attribution (CC BY) license (<https://creativecommons.org/licenses/by/4.0/>).

Keywords: multistage classifier; binary tree; artificial neural network; support vector machine; classification; HEp-2; IoMT

1. Introduction

Sustainable smart cities [1] incorporate a range of innovations for automation, data sharing, and distribution that transform the environment of how we produce goods. In

terms of how goods are made, the world is in the middle of a massive transition. This transformation is so convincing that the fourth revolution has taken place in numerous technological applications, such as the medical sector [2]. The IoT integrates embedded hardware, applications, sensors, and network communication with physical objects, which ensures they can capture and share data. This is the Industrial IoT (IIoT) [3] with added machine learning, machine-to-machine connectivity, and incorporation of current automated systems. To make the right manufacturing decisions, smart computers can reliably collect real-world data and interact with one another and the goods or resources they are handling. In terms of delivering reliable diagnostic instruments, medical device manufacturers are facing growing difficulties. The area of automated diagnostics and artificial intelligence in medical diagnosis has made significant strides in recent years. One of the experiments demonstrated the use of feature selection and parameter optimization in Artificial Neural Networks (ANN) to automate breast cancer diagnosis [4]. The resolution of complex medical diagnoses using pattern recognition requires an artificial neural network-based expert system for the automation of autoimmune disease diagnoses in the blood samples. Antinuclear antibody (ANA) tests identify and classify the existence of auto-antibodies in the blood serum that bind to antigens found in the nuclei of mammalian cells. The Indirect Immunofluorescence (IIF) technique is used in the ANA test with HEp-2 cells as substrates. Pathologists [5] observe this IIF slides to build their study. As the home-based chronic disease monitoring is gaining popularity these days, the automation of autoimmune disease diagnosis through the antinuclear antibody (ANA) technique is proposed in this work, for which a Multistage Classification Scheme (MSCS) is developed using image-based Computer-Aided Diagnosis (CAD), for improving the process standard. Most of the work in the literature has used deep learning techniques, whose accuracy relies on the huge size of the dataset and the need to optimize too many parameters, which require high-end machines for training. This study classifies HEp-2 cells in three stages by using Binary Tree (BT), ANN, and Support Vector Machine (SVM) as basic blocks. The first stage predictions, along with the most suitable spectral, statistical, and spectral descriptors, are used as novel feature set for HEp-2 cell classification. In the proposed approach, initially the intermediate and positive cells are segregated followed by which preprocessing is performed for dark and low contrast intermediate cells and the positive cells. In the first stage of classification, the base learners BT1, ANN1, and SVM1 are trained individually with only spectral, statistical, and textural descriptors (24 features). The selected 24 features are: standard deviation of the cell image; area of the cell in the binary image; ratio of standard deviation to area; the number of objects in the cell using eight adjacency connectivity; contrast of co-occurrence matrix; correlation of co-occurrence matrix; energy of co-occurrence matrix; homogeneity of co-occurrence matrix; the first six eigenvalues of principal component analysis for the Fast Fourier Transform of an eight-window Local Binary Pattern histogram; average power spectral density of the LL subband; LH subband; HL subband; HH subband; and the first six eigenvalues of principal component analysis for the cell image. In the second stage, the meta learners BT2, ANN2, and SVM2 are again trained for the augmented feature set obtained by combining the first stage prediction results along with the 24-element feature set. The positive and intermediate cells are combined in the second stage. In the third stage, the results of the BT2 ANN2 and SVM2 are ensembled using majority voter logic. The efficiency of the proposed methodology is assessed using the dataset of ICPR 2016 [6]. The results concluded that the MSCS method achieved the mean class accuracy of “99.1%” efficiency. However, the effectiveness of the proposed approach is further improved with the advent of Internet of Medical Things (IoMT) based digital pathology [7]. This technique provides remote health monitoring, with the help of clinical gadgets linked to cloud and wireless network resources, and offers efficient solutions to patients to monitor and assess their health conditions and provide feedback from distant facilities in critical pandemic conditions like COVID-19. Healthcare informatics require computational intelligence [8] and visualization for scientific research. Tozzoli et al. [9] reviewed the most important changes that have occurred in autoimmune diagnostics. Many diseases require disruptive

technologies [10] to perform analysis and scientific research. Healthcare professionals have various challenges while treating patients during a pandemic. The patient's health is monitored through IoMT technology. Depending on the results, unique safety measures might be put into place. It is crucial to the healthcare industry's efforts to improve the accuracy, reliability, and efficiency of electronic devices. IoMT can connect genuine, physical items in the real world for information sharing and communication. Additionally, it ensures the caliber of the service. Simple communication protocols are used to follow biological signals for diagnosis. IoMT-based digital pathology focuses on data management based on information generated from digitized specimen slides using virtual microscopy. It uses an image-based environment that enables the acquisition, management and interpretation of pathology information generated from a digitized glass slide. This requires a unit to be deployed in remote clinics where field workers would prepare blood samples for inspection. With the aid of an IoT-enabled microscope, the blood smear images are uploaded to the cloud network for diagnosis. To automate the diagnosis, the proposed MSCS identifies the microscopic images, where regions-of-interest (ROI) are identified for high-resolution tissue scans and diagnose the results of the autoimmune disorder. In this work, the IoMT allows for effective scheduling of limited resources for the automated diagnosis of autoimmune diseases by ensuring the best use of resources while serving the maximum number of patients. The clinical team may make judgments that decrease medical mistakes using this wide range of accurate wellness data. Active aging, population monitoring, healthy lifestyles, care service organization, and emergency response were considered to be the applications most suitable for implementation. This data may be used to decrease the response time for illness detection and patient comfort by quickly providing crucial information. IoMT's most significant contributions to the pandemic response come from effective data management, first-rate treatment, and improved diagnostics. We delineate our experiments in the following sections. The results of the research work are mentioned in Section 2. Related work is presented in Section 3. Section 4 discusses the methods and materials required for IoMT-based automation of autoimmune diagnosis using MSCS, with appropriate results discussed in Section 5. Section 6 shows the comparison of the proposed approach with the state-of-the-art methods. Section 7 draws the final conclusions for future work.

2. Contributions

The contributions of the proposed work are listed below:

- The proposed feature set was based on the first stage classification results, which showed less within-class variance and more between-class variance as compared to well-known spectral, statistical, and textural features, which made them the best predictors for classification problems.
- The images in the dataset were separated into low-information and medium-information images based on the average intensity and contrast, and special preprocessing was applied for low-information images, which will eventually increase the performance of the classification task.
- Unlike CNN, the data augmentation and optimization of many parameters were not required.
- The architecture can be applied to complicated texture-based multiclass classification problems.

3. Related Works

This section addresses the research and different approaches used in the field of HEp-2 cell classification along with the accuracy results achieved.

Khan et al. [11] defined the essential features involved in the prediction of heart disease. In this work, IoMT architecture for diagnosing heart disease with updated salp swarm optimization (MSSO) and an adaptive neuro-fuzzy inference method (ANFIS) is proposed by the authors to improve prediction accuracy. Work by Basatneh et al. [12] studied the possible

issues involved in the application of IoMT for DFU management. A mobile cloud-based IoMT scheme was deployed by Nguyen et al. [13] to track the progression of a neurological condition using a muscle control test. The cloud server's computational and storage capacities are used to promote the calculation of the severity levels provided by a defined quantitative evaluation. For data collection and collaboration with the cloud, an Android framework is used. In a blockchain network, the authors have combined the proposed system into a data-sharing platform as a revolutionary approach that enables healthcare consumers to share data reliably. In a wide variety of healthcare applications, an illustration of IoMT application for orthopaedic treatment is discussed by Singh et al. [14], where the possibility of confronting the autoimmune diseases is also discussed. Numerous cloud and network-based facilities of IoMT are data sharing, report reporting, patient tracking, knowledge processing and analysis, hygiene medical treatment, etc. When treating orthopedic patients with a higher quality of treatment and more satisfaction, it can comprehensively change healthcare facilities' functional layout. With the proposed IoMT method, remote-location healthcare is possible. IoT coordination protocols for their use in IoMT are classified by Koutras et al. [15]. In this work, the authors define the key features of IoT communication protocols used in medical device vision, network, and application layer. Further, the intrinsic security properties of IoMT-specific communication protocols and their drawbacks are also discussed. Additionally, the authors define available mitigation controls that can be added to secure IoMT communications and current analysis and deployment gaps, based on practical threats. Knowledge, versatility, and interoperability will be greatly improved by incorporating IoT solutions into healthcare systems. A comprehensive survey on evolving IoT connectivity norms and innovations relevant for smart healthcare applications was given by Gardasevic et al. Low-power wireless technology as a vital enabler for energy-efficient IoT-based healthcare systems that have been given particular importance. Major privacy and protection issues are also addressed. Finally, the complexities of open science and future IoMT insights are discussed. Foggia P. et al. [16] examined the approaches published at the 2012 International Conference on Pattern Recognition, the HEp-2 Cells Classification contest. Similarly, a system for HEp-2 cell classification was recommended by William et al. [17] using a dual-region codebook-based descriptor along with the Closest Convex Hull Classifier. An overall classification accuracy of $95.5 \pm 2.2\%$ was obtained by the HEp-2 cell classification using a dual-region codebook-based descriptor and NCH.

The work by Pasquale Foggia et al. [18] compared the experimental outcomes, and identified the advantages and drawbacks of each strategy. They noticed that characteristics dependent on texture were promising.

Through conducting studies on many most used function sets, V.Snell et al. [19] spotlight the shortcomings of existing methods for HEp-2 cell classifications. Just 52.3% of DCT-based descriptors, 56.5% of pixel variations alone, 52.2% of morphology features, and 35.3% of MCA were acquired through co-occurrence features.

Work by Ilias et al. [20] that combined two descriptors into a space of dissimilarity, which produced classification results of 75.1% and 85.7% at the cell and image levels.

X. Qi et al. [21] proposed a new Gaussian Scale Space (GSS) preprocessing method for the role of HEp-2 cell classification and achieved 82.03% efficiency.

A two-level pyramid technique was proposed by Donato Cascioa et al. [22] to retain certain spatial details. A broad feature of 216 was extracted using several class-process method forms. Centered on the one-against-one system, an ensemble of 15 SVM was used. On a blind Hep-2 cell dataset executing MCA equivalent to 80.12%, the classification scheme was tested. The use of IoMT in healthcare has exploded around the world, but it still faces many technological and design challenges. Turjman et al. [23] represented those problems and demonstrated a generic IoMT architecture to address them, which consists of three key components: data collection, connectivity gateways, and servers/cloud. A Deep Learning Model Inception V3 and Xception architectures were used for classification of Hep-2 cells and obtained an accuracy of 95.07% [24]. Linear discriminant analysis was used for feature extraction and kernel support vector machines as well as fuzzy C-means

were employed for fast classification of specimens and achieved mean class rates (MCAs) of 86.02% and 89.14%, respectively [25].

Compared with the discussed studies, the proposed MSCS based architecture is different from those discussed in this section in the following ways:

- First stage classification uses BT1, ANN1, and SVM1, which are also proved as suitable features for the second stage performance results.
- Considering the performance, three-stage classification architecture was implemented, which does not require data augmentation and many parameter optimizations.
- Special preprocessing was applied for dark and low contrast intermediate cells to enhance the image information after segregating from positive cells based on average intensity instead of common preprocessing for intermediate and positive cells.

4. IoMT-Based Automation of Autoimmune Diagnostics using MSCS: Methods and Materials

This section presents an IoMT-based system for automating the detection of autoimmune diseases through the antinuclear antibody (ANA) test in this paper. The proposed IoMT framework is shown in Figure 1.

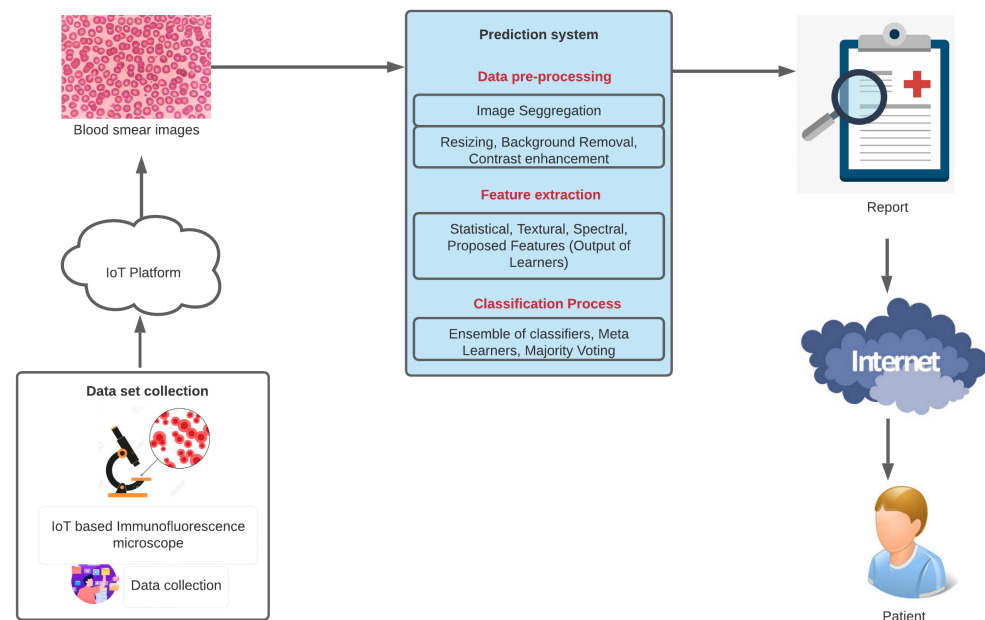


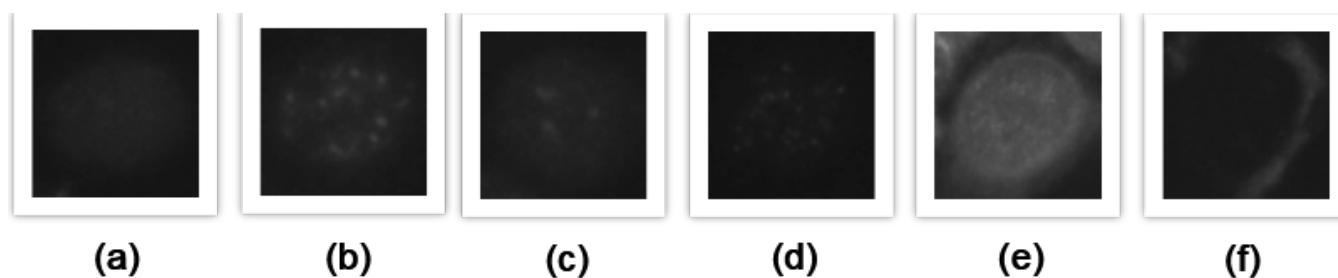
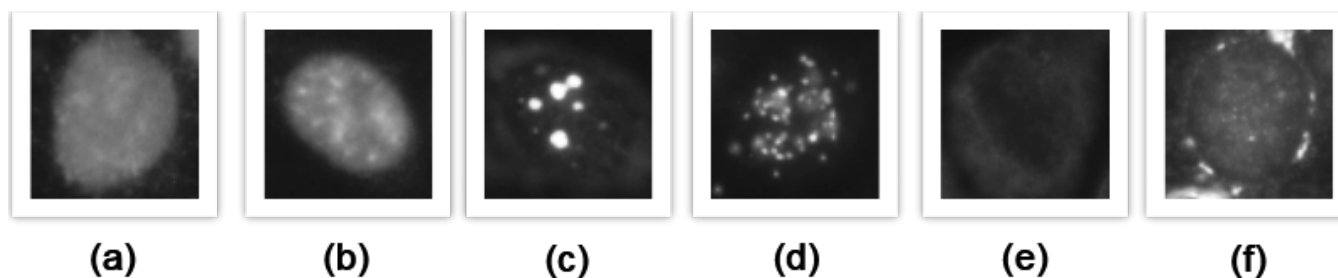
Figure 1. IoMT-based framework for the automation of autoimmune disease diagnosis.

The Indirect Immunofluorescence (IIF) technique used for the reading and interpretation of antinuclear antibody test with HEp-2 cells as substrates, is developed and tested on the dataset [6] using IFF as the reference method for ANA. Pathologists observe this IIF slides to build their study. As the home-based chronic disease monitoring is gaining popularity these days, the automation of autoimmune disease diagnosis [26] through the antinuclear antibody (ANA) technique is proposed in this work, for which a Multistage Classification Scheme (MSCS) is developed using image-based Computer-Aided Diagnosis (CAD), for improving the process standard. This study classifies HEp-2 cells using 13,596 cell images.

Initially, these images are manually segmented and categorized by experts. Six staining patterns are seen in the images as shown in Figure 2 as well as Figure 3. The summary of the HEp-2 ICPR 2016 dataset is shown in Table 1.

Table 1. Summary of HEP-2 ICPR 2016 dataset.

Pattern	# of Intermediate Cells	# of Positive Cells	# of Cells
Homogeneous	1407	1087	2494
Speckled	1374	1457	2831
Nucleolar	1664	934	2598
Centromere	1363	1378	2741
Nuclear membrane	1265	943	2208
Golgi	375	349	724
Total	7448	6148	13596

**Figure 2.** Sample cells from intermediate dataset [27]: (a) homogeneous, (b) speckled, (c) nucleolar, (d) centromere, (e) nuclear membrane, and (f) Golgi.**Figure 3.** Sample cells from positive dataset [27]: (a) homogeneous, (b) speckled, (c) nucleolar, (d) centromere, (e) nuclear membrane, and (f) Golgi.

4.1. Multistage Classifier Scheme for HEP-2 Cell Classification

The overview of the proposed architecture for the HEP-2 cell pattern classification was shown in Figure 4. Firstly, the proposed technique splits the positive cells and intermediate cells based on the image's overall average intensity before preprocessing. This results in darker and low contrast intermediate cell images with less spatial information when compared to positive cells. Following this, separate preprocessing is done for intermediate and positive cells for better accuracy. The hybrid feature set (24 elements) of textural (4 + 6), statistical (4 + 6), and spectral features (4) were extracted. As HEP-2 cell images had microtextures, texture descriptors were well-suited. The proved textural descriptors such as Gray level co-occurrence matrix (GLCM) and Local Binary Pattern (LBP) were used. Four statistical properties of GLCM were extracted, as these had good discriminating properties for HEP-2 cells. LBP was rotation variant, Fast Fourier Transform (FFT) was applied on LBP to make it almost rotation invariant. Dimensionality reduction using Principal Component Analysis (PCA) had a great advantage, as the FFT of LBP was 256 values. The number of training cell images of Golgi's pattern was only 375 for intermediate and 349 for positive. Here, dimensionality reduction would avoid overfitting errors. So, PCA was applied to the FFT values of LBP to obtain the first six eigenvalues. In total, ten textural descriptors were considered for the present classification problem. The grayscale image of cells was transformed into a binary image. The statistical properties of the cell area and the number

of objects were calculated on the binary image. The standard deviation of the grayscale cell image and standard deviation by area were also estimated for the cell image. The area of the cell varies significantly among the patterns. The homogenous, nuclear membrane, and speckled had more area than centromere, Golgi, and nucleolar. The standard deviation of the cell image varied a lot among the patterns, as standard deviation measures the degree of nonuniformity of the pixel values concerning the space in the image. The number of objects in the image was a very simple but effective discriminator. As homogenous patterns, the nuclear membrane had few objects, and centromere, speckled, and Golgi had more objects than the nucleolar pattern. PCA of the cell image was a statistical property that represents the whole image pixels in the form of an uncorrelated orthogonal basis set. PCA was a suitable feature for HEp-2 cells as the cell image patterns had variations in the pixel value distribution. The first six eigenvalues of the PCA were significant. Totally ten statistics features were considered for the classification problem in hand. Spectral features of the HEp-2 cell showed a significant difference among the patterns, as pixel values of the patterns were randomly distributed with significant variations. High frequencies represented the abrupt intensity changes like edges of the object, and low frequency represented the slow variations in the intensity. Low Low (LL), High Low (HL), Low High (LH), and High High (HH) features were extracted using Discrete Wavelet Transform had good discriminating characteristics. Only four spectral features were taken for the classification task.

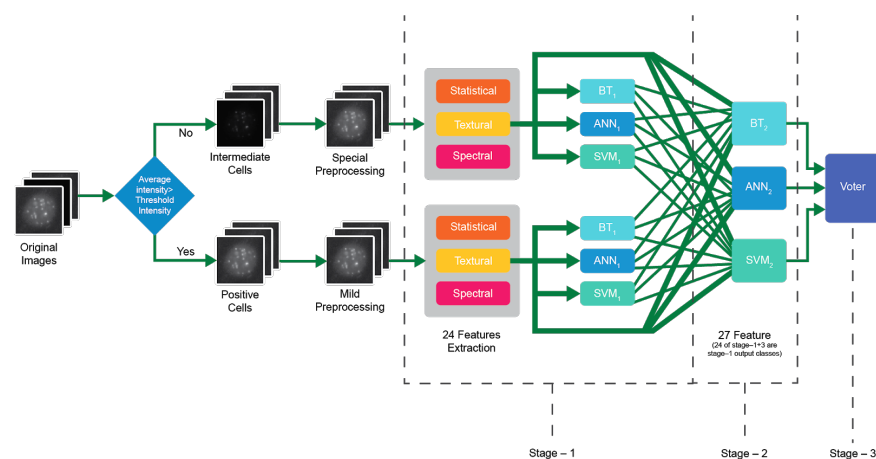


Figure 4. An overview of the Multistage Classifier Scheme for classification of HEp-2 cells.

The BT was a suitable classifier for the HEp-2 cell segregation problem as the team of cell patterns share the common values in the view of certain features. For instance, homogenous, nuclear membrane, and speckled had more area than centromere, Golgi, and nucleolar, so six patterns could be grouped into two based on the cells' area. Similarly, suitable features were identified, and HEp-2 cells were segregated. More details were discussed in section C.

ANN was also an appropriate classifier for the HEp-2 cell categorization problem. The HEp-2 cell classification problem is considered a complex classification problem because the intraclass variations are more. ANN can handle such issues by adjusting the weights by the more sophisticated algorithms like scaled conjugate gradient back propagation (SCGBP) during the training process. SVM was considered as a suitable classifier [28]. The BT, ANN, and SVM were base classifiers. In the proposed Multistage Classification Scheme (MSCS), BT1, ANN1, and SVM1 were trained individually with only 24 On the image training datasets in the first stage as base learners. In the second stage, the feature set was augmented to 27 elements with the first stage prediction results again meta learners BT2, ANN2, and SVM2 were trained for this augmented feature set to achieve better accuracy. Both intermediate as well as positive cells feature set are combined to produce a prediction class. The first stage prediction results had significantly less intraclass variance and good inter-class variance. Thus, the performance of classification increases in the

second stage of the classification. In the third stage, the results of the BT2, ANN2, and SVM2 were combined using majority voter logic to produce a predicted class. The majority voter logic was appropriate, as the instances with different prediction results from the three classifiers were lower. To validate the efficiency of the proposed architecture, the leave-one-specimen-out validation scheme has been modified.

4.1.1. Preprocessing

Contrast stretching is used in this stage because of the low contrast in intermediate cell images. This is achieved by preserving the lowest possible value of the image intensity, while the highest possible value is set to the maximal possible value of the intensity. Using morphological structuring feature, the context is removed to highlight the cell structure in the picture and the image size is converted into a resolution of 64×64 . This resolution is translated to 64×64 for positive cells and the backdrop is deleted.

4.1.2. Feature Extraction

Extraction of features codes broad image data into a condensed form. Inter-class variation features like spectral, statistical and textural are considered for the cell classification. Among these, textural descriptors have important segregation features [16,18]. Mathematical, textural, and spectral as well as first stage predictions used for the classification of HEp-2 cell images include:

- **Statistical features (Stat):** A valuable representation of data for study can also be conveniently derived from the statistical functionality. The number of “one” pixels in the binary picture is the area of the cell. Any information about the dispersion of the intensity in the cell is given by the standard deviation of the picture. For the HEp-2 cell classification, the number of items in the cells was also an excellent discriminating feature.
- **Principal component Analysis (PCA):** Is a statistical approach that utilizes orthogonal transformation to convert results. For Cell Image, the PCA was applied. For the Feature Set, the first six eigenvalues are taken.
- **Textural features (text):** The texture is described in the neighborhood by the spatial distribution of gray levels [29]. The literature review noted that for the classification task, textural descriptors were more useful.
- **Statistics of co-occurrence matrix (SCM):** Microtextures are seen in HEp-2 cell images. As a micro-texture descriptor [29], a gray-level co-occurrence matrix was well matched. The distribution of co-occurring values over an image at a given offset was calculated by the co-occurrence matrix (CM). The statistical properties were measured over the CM, such as homogeneity, comparison, correlation, and energy. Consequently, for one-pixel distance CM, the feature set had four components.
- **Principal Component Analysis of Local Binary Pattern histogram frequency response (PCALBP) [27]:** One of the important ways to explain texture is the Local Binary Pattern (LBP). The neighborhood is thresholded relative to the center pixel value. The function set has six parts.
- **Power Spectral Components(PSC) [27]:** Using the wavelet function’s decomposition property, the classification accuracy can be improved. For the dataset [27], the interaction between the features of sub-bands was technically tested and simulated.

4.2. Classifiers

- **Binary tree (BT):** The conditional decision tree has “true” or “false” formal outputs. In the HEp-2 cell pattern recognition problem [30], BT is used as a classifier. BT was a supervised algorithm for learning. In which, the predictors of the training images were analyzed using the Classification and Regression Trees (CART) algorithm to perform a binary split on any predictor variable. The split criterion gain was determined according to the CART algorithm by the ratio of the parent to child node Gini diversity index [30]. The minimum leaf size at which the tree’s output was optimum is the

minimum observations on the leaf node. In this experiment, the minimum leaf node size set was 50. Tree splitting ends until the minimum leaf size is met by the number of observations on a leaf.

- **Artificial Neural Network (ANN):** ANN [31] is comparatively one of the better choices for complex classification of HEP-2 cell patterns. With ten layers, the ANN design adopted the feed-forward strategy. During the preparation of the ANN, scaled conjugate gradient backpropagation [32] was used to change the weights. Hyperbolic tangent sigmoid, hyperbolic log sigmoid, and softmax were alternatively implemented in the transition function.
- **Support Vector Machine (SVM):** SVM adopted the guided learning methodology. SVM was a binary classifier, essentially. The binary SVM was modeled to classify six groups using the Error-Correcting Output Code. Therefore, $\frac{K(K-1)}{2}$ was used, i.e., fifteen SVMs, where K is the number of groups. A Gaussian kernel one-versus-all coding scheme was used.
- **Multistage Classification Scheme (MSCS):** The Multistage Classification Scheme is proposed by keeping performance improvement as an ultimate goal. The proposed MSCS retrains the base classifiers to improve the predictive accuracy in computer vision problems. The MSCS algorithm is shown in Algorithm 1.

Algorithm 1: MSCS Algorithm

Input: The dataset $S = \{L_n, F_n\}$, $n = 1 \dots N$, where L_n is the class label, F_n represent the feature set for the cell n and $N=13596$

Output: Predicted class

- Step 1:** Segregate the intermediate S_i and positive S_p HEP-2 cells based on the average intensity.
- Step 2:** Special preprocessing for intermediate cells S_i and mild preprocessing for positive cells S_p .
- Step 3:** Extract spectral, statistical and textural features (24 features) for both S_i and S_p .
 $S_i = \{L_{n_i}, F_{n_i}\}$, $n_i = 1 \dots N_i$, where, L_{n_i} was the class label, F_{n_i} represent the feature set for the intermediate cell n_i and $N_i = 7448$. $S_p = \{L_{n_p}, F_{n_p}\}$, $n_p = 1 \dots N_p$, where L_{n_p} is the class label, F_{n_i} represent the feature set for the positive cell n_p and $N_p = 6148$.
- Step 4: MSCS-Stage-1** Base learner BT_1 , ANN_1 , and SVM_1 were trained with 24 features separately for S_i and S_p . For instance x_i cell in S_i , $P_{f_{i1}}$, $P_{f_{i2}}$, and $P_{f_{i3}}$ denote the prediction of the base classifier BT_1 , ANN_1 , and SVM_1 , respectively.
- Step 5: MSCS-Stage-2** Meta learners BT_2 , ANN_2 , and SVM_2 were trained with augmented feature set Z (27 features = 24 features + 3 outputs of base classifiers). Intermediate and positive cells were combined Let $Z_x = \{P_{f_{i1}}, P_{f_{i2}}, P_{f_{i3}}, F_x\}$, $x \in S$, Where $P_{f_{i1}}$, $P_{f_{i2}}$, and $P_{f_{i3}}$ denote the prediction of the base classifier BT_2 , ANN_2 , and SVM_2 , respectively, for the cell x . Now, dataset $S_Z = \{X_n, Z_n\}$, $n = 1 \dots N$ where Z_n is the class label and X_n is the augmented feature set for the cell n and $N = 13596$.
- Step 6: MSCS-Stage-3** The output of meta learners P_{s_1} , P_{s_2} , and P_{s_3} were an ensemble using the majority voting technique as shown in Equation (1).

$$Maj\{P_{s_1}, P_{s_2}, P_{s_3}\} = P \quad (1)$$

where P is the final predicted class.

if $P_{s_1} \neq P_{s_2} \neq P_{s_3}$, then $P_{s_1} = P$ as BT_2 has more performance than other classifiers. This increases the performance of the classification system.

5. Results and Discussion

The proposed architecture for HEp-2 cell classification using mathematical, textural, and spectral characteristics using MSCS is evaluated in this section on the dataset [27]. The MCA was defined as shown in Equation (2).

$$MCA = \frac{1}{k} \sum_{i=1}^k CA_i \quad (2)$$

where CA_i is the classification precision of class i , and k is the number of groups of cells. ACA is the correct average classified cells in the dataset for the complete cells. Out of 13,596 cells in the full dataset, the intermediate cells (IMC) were 7448 (54.8%), as it was the plurality of size, special consideration yields greater precision of classification. 6148 (45.2%), which were of medium knowledge, were the positive cells (PC). To produce the uncertainty matrix, a leave-one-specimen-out validation protocol was used.

5.1. Stage 1 Results

The IMC and PC were separated in Stage 1 prior to preprocessing on the basis of their total strength, and special preprocessing is applied to intermediate cells for improved output, and positive cells are subjected to mild preprocessing. The statistical, textural, and spectral features were extracted to form a feature set with 24 elements. The intermediate cells were darker and had low contrast. Even after special preprocessing, the intermediate cells had less spatial information. The MCA is 84.9% for intermediate cells, although the carefully picked 24 features and SVM classifier were applied. The MCA is 95.8% for positive cells for the same feature set and SVM classifier, as positive cells had comparatively good spatial information. ANN is better for intraclass varying HEp-2 cell pattern classification as it can handle the intraclass variations by adjusting the weights using the SCGBP algorithm. So, the MCA is 88.4% and 97.1% for intermediate and positive cells, respectively. BT is more suitable for this kind of segregation problem, as the few cell patterns share the common values in the view of certain features; this allows us to group the patterns based on such features. So, the MCA is 95.3% for intermediate and 98.6% for positive. The base learners were trained for these 24 elements, and leave-one-specimen-out validated to obtain the MCA, as shown in Table 2 and Figure 5.

Table 2. Results of Stage 1.

Classifier	BT			ANN			SVM			
	Dataset	IMC	PC	Combined	IMC	PC	Combined	IMC	PC	Combined
MCA		95.30%	98.60%	96.80%	88.40%	97.10%	92.40%	84.90%	95.80%	89.80%

For further understanding, the majority voting algorithm was implemented after Stage 1 to ensemble the classifiers' output. The majority voting technique was chosen as an ensemble method because 99.08% of the instances were voted by at least two of the classifiers, and it is simple to implement. Table 3 summaries the input and output of the voting algorithm at Stage 1. For 115 cases, the prediction results of BT, ANN, and SVM were different.

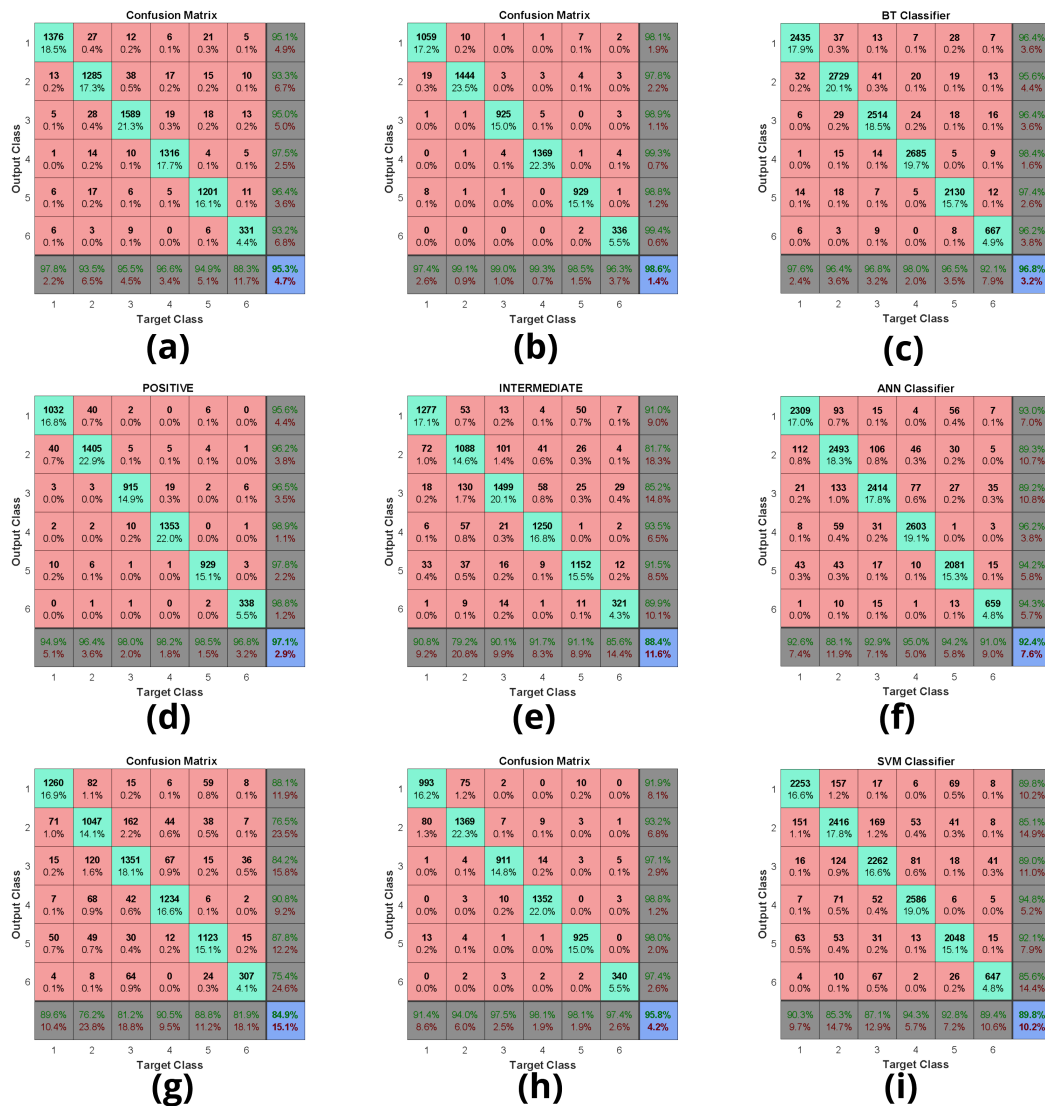


Figure 5. Confusion matrix results of Stage 1: (a) Intermediate BT_1 , (b) positive BT_1 , (c) intermediate and positive combined BT_1 , (d) intermediate ANN_1 , (e) positive ANN_1 , (f) intermediate and positive combined ANN_1 , (g) intermediate SVM_1 , (h) positive SVM_1 , and (i) intermediate and positive combined SVM_1 .

Table 3. Input and output of the voting algorithm at Stage 1.

Voter at Stage 1	BT, ANN, SVM Vote Same Class	ANN, SVM Vote Same Class	BT, ANN Vote Same Class	BT, SVM Vote Same Class
Correct prediction	11709	451	616	313
Wrong prediction	107	199	27	59
Total	11816	650	643	372

5.2. Stage 2 Results

In Stage 2, the Meta learners BT_2 , ANN_2 , and SVM_2 were trained for an augmented feature set (24 + 3 results from base learners). The base learners' predicted results had significantly less intraclass variance and more inter-class variance, making a good feature for the classification. Therefore, the performance of BT_2 , ANN_2 , and SVM_2 was increased by 1.8%, 4.5%, and 4.1% as compared to Stage 1, as shown in Figure 6.

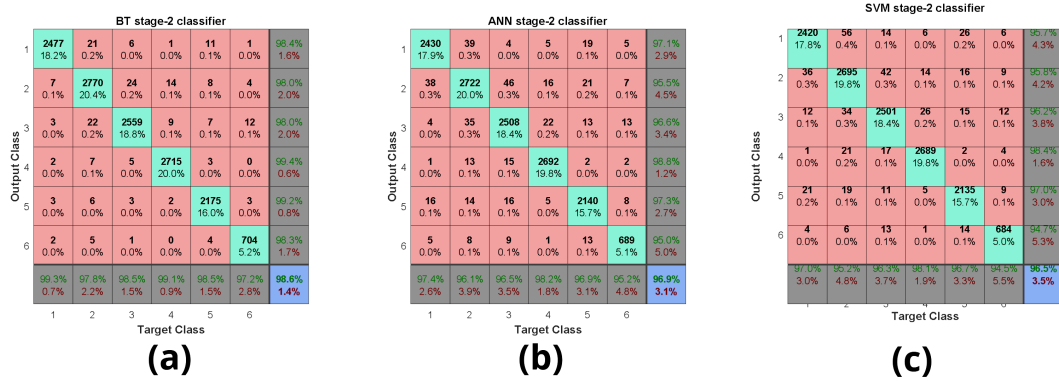


Figure 6. Confusion matrix results of Stage 2: (a) BT₂ result, (b) ANN₂ result, and (c) SVM₂ result.

5.3. Stage 3 Processing and Results

In Stage 3, the final prediction was performed by majority voting among the results of the three meta learners to achieve 99.1% MCA, as shown in Figure 7. Majority voting was a suitable method for ensembling the results, as there were very few instances with different results for all three classifiers. Homogenous (Class-1) had the highest performance, with 99.6% (2484), and Golgi (Class-6) had a lower performance of 98.2% (711). The results of the proposed MSCS are summarized in Table 4.

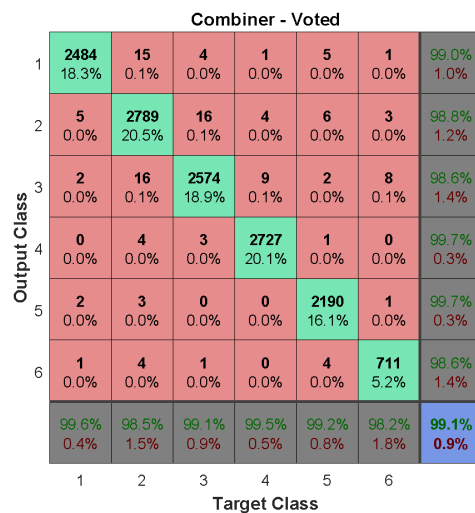


Figure 7. Confusion matrix results of Stage 3.

Table 4. Results of Stage 2 and Stage 3.

Classifier	Stage 2			Stage 3
	BT	ANN	SVM	Voter
MCA	98.60%	96.90%	96.50%	99.10%

6. Comparison with State of Art Methods

The technique used by Manivannam et al. [33] for HEP-2 Cell recognition with an MCA of 87.9% on the dataset uses spatial relationship-based linear coding and two-level cell pyramids to encode different characteristics to reflect the spatial details of the cells. The MCA of 93.7% was obtained by Sadaf et al. [34] for the ICPR 2014 dataset [27] using the leave-one-specimen-out validation protocol. Deep Convolution Neural Networks were proposed by ZGao [35] (d-CNN) for HEP-2 cell classification. The architecture of the d-CNN consisted of eight layers; the first six layers were every other convolution and pooling layers. The rest of the two layers were fully connected layers designed for classification.

The first layer of the classification takes the sixth layer output feature map as input. The last layer gives the output probabilities using the softmax regression model by optimizing weights and biases.

The d-CNN cost function was nonconvex, so it requires setting many training parameters approximately 50,000 for the fast network converge and good performance. As more parameters need to be optimized for d-CNN during training, more training images were a must. So, cell image rotation based data augmentation technique is one way to achieve more images from the dataset. This makes d-CNN more computationally complicated [36], have more running time, and consume more memory. The proposed multi-stage classifiers do not require data augmentation, so they consume less memory and are computationally less complicated, as fewer parameters need to be optimized. A 22 layered CNN with four pooling layers and three classification layers was used by Xi Jia et al. [12]. This produced MCA 85.1% on the dataset [27].

On the image training dataset [27], the proposed architecture achieved an MCA of 99.1%. The training data collections [27] are the same as seen in Table 1. The state of the art processes are shown in [27]. The proposed MSCS technique has outperformed the ensemble of convolutional neural networks [24], which gave an accuracy of 95.07%, and a linear discriminant analysis technique [25], which gave an accuracy of 89.14%.

7. Conclusions and Future Work

By facilitating access to healthcare for citizens' well being, a sustainable smart city can better guarantee health care. This work focused on the automation of autoimmune disease diagnosis through the antinuclear antibody (ANA) technique using the MSCS approach. Pattern recognition architecture for complex HEp-2 cell classification is developed and tested on the dataset [27]. One of the most effective classification systems has been found to be the MSCS for classification. In this research work, a pattern recognition architecture for a complicated classification task was designed and tested on the ICPR 2016 HEp-2 dataset. The MSCS for classification proved to be one of the most efficient schemes. In the output stage, the output of all three meta-learners was combined by the majority voting technique to give an accuracy of 99.1%. The ANA test with the IIF method is the gold standard for diagnosing auto-antibodies in the blood serum. ANA testing is subjective with more inter-laboratory variations due to the lack of specialized personnel. The proposed algorithm can be embedded in a CAD system designed for texture-based computer vision pattern recognition problems. To improve the effectiveness of the proposed approach an Internet of Medical Things (IoMT) based digital pathology approach is introduced in this work to monitor and assess the patients' health conditions in critical pandemic conditions like COVID-19.

Author Contributions: Conceptualization, D.B.S.; methodology, D.B.S. and T.S.; software, D.B.S. and T.S.; validation, D.B.S. and F.A.-T.; formal analysis, D.B.S. and F.A.-T.; investigation, M.K.; resources, M.K.; data curation, S.A.; writing—D.B.S.; writing—review and editing, D.B.S., T.S.; supervision, F.A.T. and S.A.; project administration, M.K. and S.A.; funding acquisition, M.K. and S.A. All authors have read and agreed to the published version of the manuscript.

Funding: This research received no external funding.

Institutional Review Board Statement: Not applicable.

Informed Consent Statement: Informed consent was obtained from all subjects involved in the study.

Data Availability Statement: Not applicable.

Conflicts of Interest: The authors declare no conflict of interest.

References

1. Pacheco Rocha, N.; Dias, A.; Santinha, G.; Rodrigues, M.; Queirós, A.; Rodrigues, C. Smart cities and healthcare: A systematic review. *Technologies* **2019**, *7*, 58. [[CrossRef](#)]
2. Ghazal, T.M.; Hasan, M.K.; Alshurideh, M.T.; Alzoubi, H.M.; Ahmad, M.; Akbar, S.S.; Al Kurdi, B.; Akour, I.A. IoT for smart cities: Machine learning approaches in smart healthcare—A review. *Future Internet* **2021**, *13*, 218. [[CrossRef](#)]
3. Suresh, A.; Nandagopal, M.; Raj, P.; Neeba, E.; Lin, J.W. *Industrial IoT Application Architectures and Use Cases*; Auerbach Publications: Boca Raton, FL, USA 2020.
4. Punitha, S.; Al-Turjman, F.; Stephan, T. An automated breast cancer diagnosis using feature selection and parameter optimization in ANN. *Comput. Electr. Eng.* **2021**, *90*, 106958.
5. Hartman, D.J.; Pantanowitz, L.; McHugh, J.; Piccoli, A.; OLeary, M.; Lauro, G.R. Enterprise implementation of digital pathology: feasibility, challenges, and opportunities. *J. Digit. Imaging* **2017**, *30*, 555–560. [[CrossRef](#)] [[PubMed](#)]
6. ICPR Pattern recognition techniques for indirect immunofluorescence images analysis. In Proceedings of the 23rd International Conference on Pattern Recognition (ICPR 2016), Cancún, Mexico, 4–8 December 2016. Available online: <https://hep2.unisa.it/> (accessed on 18 October 2022).
7. Hosseini, M.S.; Lee, D.; Gershanik, D.; Lee, D.; Damaskinos, S.; Plataniotis, K.N. Whole Slide Preview Image Segmentation and Setup for Digital Pathology Scanners. *bioRxiv* **2020**. [[CrossRef](#)]
8. Chang, V. Computational Intelligence for Medical Imaging Simulations. *J. Med. Syst.* **2017**, *42*. [[CrossRef](#)]
9. Tozzoli, R.; D’Aurizio, F.; Villalta, D.; Bizzaro, N. Automation, consolidation, and integration in autoimmune diagnostics. *Autoimmun. Highlights* **2015**, *6*, 1–6. [[CrossRef](#)]
10. Abdel-Basset, M.; Chang, V.; Nabeeh, N.A. An intelligent framework using disruptive technologies for COVID-19 analysis. *Technol. Forecast. Soc. Chang.* **2021**, *163*, 120431. [[CrossRef](#)]
11. Khan, M.A.; Algarni, F. A Healthcare Monitoring System for the Diagnosis of Heart Disease in the IoMT Cloud Environment Using MSSO-ANFIS. *IEEE Access* **2020**, *8*, 122259–122269. [[CrossRef](#)]
12. Basatneh, R.; Najafi, B.; Armstrong, D.G. Health sensors, smart home devices, and the internet of medical things: an opportunity for dramatic improvement in care for the lower extremity complications of diabetes. *J. Diabetes Sci. Technol.* **2018**, *12*, 577–586. [[CrossRef](#)]
13. Nguyen, D.C.; Nguyen, K.D.; Pathirana, P.N. A mobile cloud based iomt framework for automated health assessment and management. In Proceedings of the 2019 41st Annual International Conference of the IEEE Engineering in Medicine and Biology Society (EMBC), Berlin, Germany, 23–27 July 2019; pp. 6517–6520.
14. Singh, R.P.; Javaid, M.; Haleem, A.; Vaishya, R.; Al, S. Internet of Medical Things (IoMT) for orthopaedic in COVID-19 pandemic: Roles, challenges, and applications. *J. Clin. Orthop. Trauma* **2020**, *11*, 713–717. [[CrossRef](#)] [[PubMed](#)]
15. Koutras, D.; Stergiopoulos, G.; Dasaklis, T.; Kotzanikolaou, P.; Glynos, D.; Douligeris, C. Security in IoMT Communications: A Survey. *Sensors* **2020**, *20*, 4828. [[CrossRef](#)] [[PubMed](#)]
16. Foggia, P.; Percannella, G.; Soda, P.; Vento, M. Benchmarking HEp-2 cells classification methods. *IEEE Trans. Med. Imaging* **2013**, *32*, 1878–1889. [[CrossRef](#)]
17. Wiliem, A.; Wong, Y.; Sanderson, C.; Hobson, P.; Chen, S.; Lovell, B.C. Classification of human epithelial type 2 cell indirect immunofluorescence images via codebook based descriptors. In Proceedings of the 2013 IEEE Workshop on Applications of Computer Vision (WACV), Clearwater Beach, FL, USA, 15–17 January 2013; pp. 95–102.
18. Foggia, P.; Percannella, G.; Saggese, A.; Vento, M. Pattern recognition in stained hep-2 cells: Where are we now? *Pattern Recognit.* **2014**, *47*, 2305–2314. [[CrossRef](#)]
19. Snell, V.; Christmas, W.; Kittler, J. HEp-2 fluorescence pattern classification. *Pattern Recognit.* **2014**, *47*, 2338–2347. [[CrossRef](#)]
20. Theodorakopoulos, I.; Kastaniotis, D.; Economou, G.; Fotopoulos, S. Hep-2 cells classification via sparse representation of textural features fused into dissimilarity space. *Pattern Recognit. Lett.* **2014**, *47*, 2367–2378. [[CrossRef](#)]
21. Qi, X.; Zhao, G.; Chen, J.; Pietikäinen, M. HEp-2 cell classification: the role of gaussian scale space theory as a pre-processing approach. *Pattern Recognit. Lett.* **2016**, *82*, 36–43. [[CrossRef](#)]
22. Cascio, D.; Taormina, V.; Cipolla, M.; Bruno, S.; Fauci, F.; Raso, G. A multi-process system for HEp-2 cells classification based on SVM. *Pattern Recognit. Lett.* **2016**, *82*, 56–63. [[CrossRef](#)]
23. Al-Turjman, F.; Nawaz, M.H.; Ulusar, U.D. Intelligence in the Internet of Medical Things era: A systematic review of current and future trends. *Comput. Commun.* **2020**, *150*, 644–660. [[CrossRef](#)]
24. Kasani, P.H.; Kasani, S.H.; Kim, H.W.; Cho, K.H.; Jang, J.W.; Yun, C.H. HEp-2 Cell Classification Using an Ensemble of Convolutional Neural Networks. In Proceedings of the 2021 International Conference on Information and Communication Technology Convergence (ICTC), Jeju Island, Korea, 20–22 October 2021; pp. 196–200.
25. Al-Dulaimi, K.; Chandran, V.; Nguyen, K.; Banks, J.; Tomeo-Reyes, I. Benchmarking HEp-2 specimen cells classification using linear discriminant analysis on higher order spectra features of cell shape. *Pattern Recognit. Lett.* **2019**, *125*, 534–541. [[CrossRef](#)]
26. Bizzaro, N.; Tozzoli, R.; Villalta, D. Autoimmune diagnostics: the technology, the strategy and the clinical governance. *Immunol. Res.* **2015**, *61*, 126–134. [[CrossRef](#)] [[PubMed](#)]
27. Divya, B.; Subramaniam, K.; Nanjundaswamy, H. HEp-2 cell classification using artificial neural network approach. In Proceedings of the 2016 23rd International Conference on Pattern Recognition (ICPR), Cancun, Mexico, 4–8 December 2016; pp. 84–89.

28. Hobson, P.; Lovell, B.C.; Percannella, G.; Saggese, A.; Vento, M.; Wiliem, A. HEp-2 staining pattern recognition at cell and specimen levels: datasets, algorithms and results. *Pattern Recognit. Lett.* **2016**, *82*, 12–22. [[CrossRef](#)]
29. Jain, R.; Kasturi, R.; Schunck, B.G. *Machine Vision*; McGraw-Hill New York: New York, NY, USA, 1995; Volume 5.
30. Divya, B.; Subramaniam, K.; Nanjundaswamy, H. HEp-2 cell classification using Binary Decision Tree approach. In Proceedings of the 2016 IEEE EMBS Conference on Biomedical Engineering and Sciences (IECBES), Jeju Island, Korea, 20–22 October 2021; pp. 507–512.
31. Paulraj, M.; Subramaniam, K.; Yacob, S.B.; Adom, A.H.B.; Hema, C. A Machine learning approach for distinguishing hearing perception level using auditory evoked potentials. In Proceedings of the 2014 IEEE Conference on Biomedical Engineering and Sciences (IECBES), Kuala Lumpur, Malaysia, 8–10 December 2014; pp. 991–996.
32. Møller, M.F. A scaled conjugate gradient algorithm for fast supervised learning. *Neural Netw.* **1993**, *6*, 525–533. [[CrossRef](#)]
33. Manivannan, S.; Li, W.; Akbar, S.; Wang, R.; Zhang, J.; McKenna, S.J. HEp-2 cell classification using multi-resolution local patterns and ensemble SVMs. In Proceedings of the 2014 1st Workshop on Pattern Recognition Techniques for Indirect Immunofluorescence Images, Stockholm, Sweden, 24 August 2014; pp. 37–40.
34. Monajemi, S.; Ensafi, S.; Lu, S.; Kassim, A.A.; Tan, C.L.; Sanei, S.; Ong, S.H. Classification of HEp-2 cells using distributed dictionary learning. In Proceedings of the 2016 24th European Signal Processing Conference (EUSIPCO), Budapest, Hungary, 29 August–2 September 2016; pp. 1163–1167.
35. Gao, Z.; Wang, L.; Zhou, L.; Zhang, J. HEp-2 cell image classification with deep convolutional neural networks. *IEEE J. Biomed. Health Inform.* **2016**, *21*, 416–428. [[CrossRef](#)] [[PubMed](#)]
36. Abdel-Basset, M.; Chang, V.; Hawash, H.; Chakraborty, R.K.; Ryan, M. FSS-2019-nCov: A deep learning architecture for semi-supervised few-shot segmentation of COVID-19 infection. *Knowl.-Based Syst.* **2021**, *212*, 106647. [[CrossRef](#)] [[PubMed](#)]